

# Vacuum structure of Toroidal Carbon Nanotubes

K. Sasaki

*Department of Physics, Tohoku University, Sendai 980-8578, Japan*

Low energy excitations in carbon nanotubes can be described by an effective field theory of two components spinor. It is pointed out that the chiral anomaly in 1+1 dimensions should be observed in a metallic toroidal carbon nanotube on a planar geometry with varying magnetic field. We propose an experimental setup for studying this quantum effect. We also analyze the vacuum structure of the metallic toroidal carbon nanotube including the Coulomb interactions and discuss some effects of external charges on the vacuum.

## I. INTRODUCTION

In recent years carbon nanotubes(CNTs) [1] have attracted much attention from various points of view. Especially their unique mechanical and electrical properties have stimulated many people's interest in the analysis of CNTs [2–4]. They have exceptional strength and stability, and they can exhibit either metallic or semiconducting depending on the diameter and helicity [5,6]. Because of their small size, properties of CNTs should be governed by the law of quantum mechanics. Therefore it is quite important to understand the quantum behavior of the electrons on CNTs. The bulk electric properties of (single-walled)CNTs are relatively simple, but the behavior of electrons at the end of a tube(cap) or metal-CNT junction is complicated and its understanding is necessary for building actual electrical devices. On the other hands, toroidal CNTs (Fullerene ‘Crop Circles’ [7]) are clearly simple because of their no-boundary shape and they can also be either metal or semiconducting properties( hereafter we use ‘torus’ or ‘nanotorus’ instead of ‘toroidal carbon nanotube’ for simplicity). Even in the torus case, quite important effect: ‘chiral anomaly’ [8], which is of essentially quantum nature, might occur.

Low energy excitations on CNTs at half filling move along the tubule axis because the circumference degree of freedom (an excitation in the compactified direction) is frozen by a wide energy gap. Hence this system can be described as a 1+1 dimensional system. Furthermore in the case of metallic CNTs, the system describing small fluctuations around the Fermi point is equivalent to the massless fermion in 1+1 dimensions. If we include gauge field, this situation can be modeled by the quantum field theory of massless fermion which couples to the gauge field through minimal coupling. This model realizes the chiral anomaly phenomenon [9–11].

The chiral anomaly is one of the most interesting phenomena in quantum field theory and has had an appreciable influence on the modern development of high energy physics [12] and of condensed matter physics [13]. The effect of the chiral anomaly on the electrons in a nanotorus appears directly as a current flow. On the other hand, it is known in solid state physics that a one-dimensional metallic ring shows the ‘persistent current [14]’ in an appropriate experimental setting. The

current originating from the chiral anomaly shows the same magnetic field dependence to the persistent current. Therefore, the persistent current is closely connected with the chiral anomaly in 1+1 dimensions. The chiral anomaly provides a deeper understanding for the persistent current as shown in the present paper.

In this paper, we examine the anomaly effect in a metallic nanotorus and discuss how such an effect can be observed experimentally. We also clarify the vacuum structure of the model regarding the gauge field as a classical field and discuss some effects of external charges situated on the metallic torus.

The organization of this paper is as follows. After reviewing quantum physics of CNTs [15], we study the case of nanotorus in section II. In section III we point out that low energy excitations on a metallic torus at half filling can be modeled by a quantum field theory of massless fermions with gauge field and construct the Hamiltonian of this system. In section IV we discuss the chiral anomaly and show how such an effect can be observed experimentally. We examine the Hamiltonian including the Coulomb interactions and analyze an effect of the Coulomb interactions on the chiral anomaly in section V. We discuss some effects of external charges in section VI. Conclusion and discussion are given in section VII.

## II. CARBON NANOTORUS

A carbon nanotube can be thought of as a layer of graphite sheet folded-up into a cylinder. A Graphite sheet consists of many hexagons whose vertices are occupied by the carbon atoms and each carbon supplies one conducting electron which determines the electric properties of the graphite sheet. The lattice structure of a two-dimensional graphite sheet is shown in Fig.1.

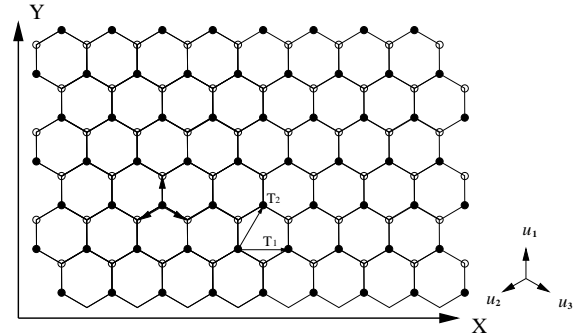


FIG. 1. Lattice structure of a two-dimensional graphite sheet ( $u_1 = ae_y$ ,  $u_2 = -\frac{\sqrt{3}}{2}ae_x - \frac{1}{2}ae_y$ ,  $u_3 = \frac{\sqrt{3}}{2}ae_x - \frac{1}{2}ae_y$ )

It is obvious, however, that this picture of a CNT as a graphite sheet rolled up to form a compact cylinder is somewhat oversimplified. We need to be careful of the following facts. First, a conducting electron makes the  $\pi$  orbitals

whose wave function extends into the Z-direction: perpendicular to the graphite sheet. Hence, in the case of multi-walled CNTs(MWCNTs), the wave functions which belong to different layers may interfere so that there is a chance that some electrical properties will alter [16] as compared with SWCNTs. Second, we should care for the curvature of a cylinder. This cause the mixing of  $\sigma$  and  $\pi$  orbital so that the band structure might change. In the present paper, we concentrate single-walled CNTs with a large diameter. Therefore the effects of interlayer interactions and curvature can safely be neglected [17].

There are two symmetry translation vectors on the planar honeycomb lattice,

$$T_1 = \sqrt{3}ae_x, \quad T_2 = \frac{\sqrt{3}}{2}ae_x + \frac{3}{2}ae_y. \quad (2.1)$$

Here  $a$  denotes the length of the nearest carbon vertex and is given by 0.142 nm.  $e_x$  and  $e_y$  are unit vectors which are orthogonal to each other ( $e_x \cdot e_y = 0$ ). If we neglect the spin degrees of freedom, because of these symmetry translations, the Hilbert space is spanned by the following two Bloch basis vectors,

$$|\Psi_{\bullet}^k\rangle = \sum_{i \in \bullet} e^{ikr_i} a_i^\dagger |0\rangle, \quad (2.2)$$

$$|\Psi_{\circ}^k\rangle = \sum_{i \in \circ} e^{ikr_i} a_i^\dagger |0\rangle, \quad (2.3)$$

where the black( $\bullet$ ) and blank( $\circ$ ) indices are indicated in Fig.1.  $r_i$  labels the vector pointing each site  $i$ , and  $a_i, a_j^\dagger$  are canonically annihilation-creation operators of the electrons of site  $i$  and  $j$  that satisfy

$$\{a_i, a_j^\dagger\} = \delta_{ij}. \quad (2.4)$$

We construct a state vector which is an eigenvector of these symmetry translations as follows:

$$|\Psi^k\rangle = C_{\bullet}^k |\Psi_{\bullet}^k\rangle + C_{\circ}^k |\Psi_{\circ}^k\rangle. \quad (2.5)$$

In order to define the unit cell of wave vector  $k$ , we act the symmetry translation operators on the state vector and obtain the Brillouin zone

$$-\frac{\pi}{\sqrt{3}} \leq ak_x < \frac{\pi}{\sqrt{3}}, \quad -\pi \leq \frac{\sqrt{3}}{2}ak_x + \frac{3}{2}ak_y < \pi, \quad (2.6)$$

where  $k_x = k \cdot e_x$ .

The mapping of the graphite sheet onto a cylindrical surface is specified by a wrapping vector:

$$C = NT_1 + MT_2, \quad (2.7)$$

which defines the relative location of the two sites. The pair of indices  $(N, M)$  describes how the sheet is wrapped to form the cylinder, and determines its electrical properties [5,6]. It can be divided CNTs into three categories depending on the pair of integers  $(N, M)$ . A tube is called ‘zigzag’ type if  $M = 0$  and ‘armchair’ in the case  $M = -2N$ . All other tubes are of the ‘chiral’ type.

To study the electronic properties of a nanotorus quantum mechanically, first we compactify the graphite sheet into

a cylinder by imposing a periodic boundary condition to the state vector. In general, we may consider the following boundary condition,

$$\hat{G}(NT_1 + MT_2)|\Psi^k\rangle = |\Psi^k\rangle. \quad (2.8)$$

$\hat{G}$  denotes a symmetry translation operator. From which we obtain

$$\frac{\sqrt{3}}{2}(2N + M)ak_x + \frac{3}{2}Mak_y = 2\pi n, \quad (2.9)$$

where  $n$  is an integer. Next, in order to make a torus, we compactify the tube into a torus by imposing a boundary condition to the tubule axis direction. For example, we may consider a ‘zigzag torus’ which has the following boundary conditions,

$$\begin{aligned} \hat{G}(NT_1)|\Psi^k\rangle &= |\Psi^k\rangle, \\ \hat{G}(M(2T_2 - T_1))|\Psi^k\rangle &= |\Psi^k\rangle. \end{aligned} \quad (2.10)$$

The former condition makes a sheet into a zigzag tube, and the latter forces the tube into a zigzag torus.

It is clear that there are many possibilities for the shape of torus and each shape has its own boundary condition. So, some of them have different properties from the one (2.10). Especially we can image a torus in which some twist exists along the tubule axis direction [18]. This system have the following boundary conditions,

$$\begin{aligned} \hat{G}(NT_1)|\Psi^k\rangle &= |\Psi^k\rangle, \\ \hat{G}(M(2T_2 - T_1))|\Psi^k\rangle &= \hat{G}(\tilde{N}T_1)|\Psi^k\rangle, \end{aligned} \quad (2.11)$$

where  $\tilde{N}$  is decided by the twist at the junction of tube end, see Fig.2. These boundary conditions yield the discrete wave vectors

$$ak_x = \frac{2\pi}{\sqrt{3}} \frac{n}{N}, \quad ak_y = \frac{2\pi}{3M} \left( m + \frac{\tilde{N}}{N} \right). \quad (2.12)$$

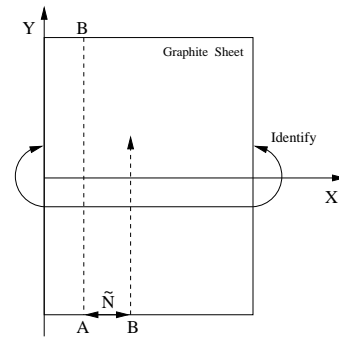


FIG. 2. Twisted zigzag torus: We impose the periodic boundary condition in the X-direction and attach same character(‘B’) in the Y-direction to obtain a twisted nanotorus. There are  $\tilde{N}$  hexagons between the point A and B.

So far we have constructed the Hilbert space of the conducting electrons. The Hilbert space is spanned by the Bloch basis vectors with the discrete wave vectors (2.12). Now, we consider the Hamiltonian which governs the time evolution of a state vector. Each carbon atom has an electron which makes  $\pi$ -orbital. The electron can transfer from any site to the nearest three sites through the quantum mechanical tunneling or thermal hopping in finite temperature. Therefore there is some probability amplitude for this process. In this case, the tight-binding Hamiltonian is most suitable:

$$\mathcal{H} = E_0 \sum_i a_i^\dagger a_i + \gamma \sum_{\langle i, j \rangle} a_i^\dagger a_j, \quad (2.13)$$

where the sum  $\langle i, j \rangle$  is over pairs of nearest-neighbors carbon atoms  $i, j$  on the lattice.  $\gamma$  is the transition amplitude from one site to the nearest sites and  $E_0$  is the one from a site to the same site. This parameter  $E_0$  only fixes the origin of the energy and therefore irrelevant. It is an easy task to find the energy eigenstates and eigenvalues of this Hamiltonian. In the matrix representation, the energy eigenvalue equation reads

$$\begin{pmatrix} E_0 & \gamma \sum_i e^{iku_i} \\ \gamma \sum_i e^{-iku_i} & E_0 \end{pmatrix} \begin{pmatrix} C_\bullet^k \\ C_\circ^k \end{pmatrix} = E_k \begin{pmatrix} C_\bullet^k \\ C_\circ^k \end{pmatrix}, \quad (2.14)$$

where

$$|\Psi_\bullet^k\rangle = \begin{pmatrix} 1 \\ 0 \end{pmatrix}, \quad |\Psi_\circ^k\rangle = \begin{pmatrix} 0 \\ 1 \end{pmatrix}, \quad (2.15)$$

and the vector  $u_i$  is a triad of vectors pointing respectively in the direction of the nearest neighbors of a black point, see Fig.1. The energy eigenvalues and eigenvectors are as follows,

$$E_k = E_0 \pm \Delta(k), \quad (2.16)$$

$$\begin{pmatrix} C_\bullet^k \\ C_\circ^k \end{pmatrix} = \frac{1}{\sqrt{2}\Delta(k)} \begin{pmatrix} \gamma \sum_i e^{iku_i} \\ \pm \Delta(k) \end{pmatrix}, \quad (2.17)$$

where

$$\Delta(k) = \gamma \sqrt{1 + 4 \cos \frac{\sqrt{3}}{2} a k_x \cos \frac{3}{2} a k_y + 4 \cos^2 \frac{\sqrt{3}}{2} a k_x}.$$

The structure of this energy band has striking properties when considered at half filling. This is the situation which is physically interesting. Since each level of the band may accommodate two states due to the spin degeneracy, the Fermi level turns out to be at midpoint of the band ( $E_k = E_0$ ). Fermi points in the Brillouin zone are located at

$$a\tilde{k}_{1,2} = (a k_x, a k_y) = (\pm \frac{2\pi}{3\sqrt{3}}, \mp \frac{2\pi}{3}). \quad (2.18)$$

Hence, if  $N$  in eq.(2.12) is a multiple of 3, then the zigzag torus shows metallic properties.

In order to understand the electric properties we should take into account a small perturbation around the Fermi point. So we take  $k = \tilde{k}_1 + \delta k$  as a small fluctuation [19]. Perturbation around the point  $\tilde{k}_2$  is same as around the point  $k = \tilde{k}_1$ . So we may only consider one of the pairs. In this case the Hamiltonian which describes the system is given by

$$-\frac{3}{2}\gamma\sigma \cdot \delta k = -\frac{3}{2}\gamma a \begin{pmatrix} 0 & \delta k_x - i\delta k_y \\ \delta k_x + i\delta k_y & 0 \end{pmatrix}. \quad (2.19)$$

This implies that the low energy excitations of metallic CNTs at half filling are described by an effective theory of two dimensional spinor obeying the Weyl equation. In coordinate space, we find

$$\mathcal{H}_{pert} = -\frac{3\gamma a}{2\hbar} \sigma \cdot p, \quad (2.20)$$

where  $p$  is the momentum operator,  $p = -i\hbar\nabla$  and  $\sigma_i$  are the Pauli matrices. It is also convenient to use a parameter  $\beta = -\frac{3\gamma a}{2\hbar}$  and  $T = \beta t$ . In this case the Schrödinger equation becomes [20]

$$i\hbar \frac{\partial}{\partial T} \psi = (\sigma \cdot p) \psi. \quad (2.21)$$

In the following section, we consider metallic and semi-conducting zigzag torus that have small  $N$  and large  $M$  values ( $\frac{M}{N} \geq 10^2$ ). In this case, transitions between different  $k_x$  are very small because of their costed energy ( $\sim \frac{|v|}{N}$ ) as compared to that of  $k_y$  ( $\sim \frac{|v|}{M}$ ). Therefore, the only surviving degree is a motion in the tubule axis direction, i.e. this system is a 1+1 dimensional system effectively.

### III. EFFECTIVE FIELD THEORY OF CARBON NANOTUBE

In this section we would like to focus on the zigzag torus which has the boundary conditions (2.10) and construct an effective field theory describing the low energy excitations in the torus. More general boundary conditions (2.11) are discussed in section IV. The zigzag torus can exhibit either metallic or semi-conducting depending on the value of  $N$ . If  $N$  is a multiple of 3 then the torus shows metallic properties. In order to analyze the semi-conducting case equally, we set  $N = \pm 3n + b$ , where  $n$  is a positive integer and  $b \in \{0, \pm 1, \pm 2\}$ . To examine the low energy excitations, we should consider the following wave vectors and energy:

$$a k_x = \pm \frac{2\pi}{3\sqrt{3}} \frac{1}{1 \pm \frac{b}{3n}}, \quad a k_y = \mp \frac{2\pi}{3} + a \delta k_y, \quad (3.1)$$

$$E_k = E_k \left( \pm \frac{2\pi}{3\sqrt{3}} \frac{1}{1 \pm \frac{b}{3n}}, \mp \frac{2\pi}{3} + a \delta k_y \right). \quad (3.2)$$

Considering the small perturbation ( $a\delta k_y < \frac{2\pi}{9}$ ) and a large diameter ( $n \geq 3$ ), the excitation energy can be approximated by

$$E_k \sim \pm \beta \sqrt{M^2 + p^2}, \quad (3.3)$$

where  $p = \hbar \delta k_y$  and

$$M = \frac{2\pi\hbar}{\sqrt{3}na} \frac{|b|}{3}. \quad (3.4)$$

Consequently, we have obtained a linear dispersion relation for metallic case ( $b = 0$ ). This is to be contrasted with the dispersion relation for semi-conducting case ( $b \neq 0$ ).

Here we comment on the excitations between different  $k_x$ . In order to neglect these excitations, we have to restrict the energy to the following region:

$$E_k < E_{\delta k_x} = \frac{\sqrt{3}\pi}{N}\gamma. \quad (3.5)$$

At room temperature, thermal excitation between different  $|\delta k_x|$  cannot occur by the Boltzmann suppression factor,  $e^{-\frac{E_{\delta k_x}}{kT}} (\sim e^{-\frac{500}{N}})$ , so that the effects of different  $|\delta k_x|$  can be ignored. Accordingly, the Hamiltonian which describes the low energy excitations near the Fermi point is given by

$$-\frac{3}{2}\frac{\gamma a}{\hbar} \begin{pmatrix} 0 & \pm M - ip \\ \pm M + ip & 0 \end{pmatrix}. \quad (3.6)$$

The sign ( $\pm$ ) in front of  $M$  comes from the  $\tilde{k}_1$  and  $\tilde{k}_2$  points. The sign can be removed by an appropriate unitary transformation of the state vector. Therefore we may choose the minus sign without loss of generality. Using the unitary transformation,  $U = e^{-i\frac{\pi}{4}\sigma_x}$ , the Schrödinger equation becomes

$$i\hbar\frac{\partial}{\partial T}\psi = \begin{pmatrix} p & -M \\ -M & -p \end{pmatrix}\psi. \quad (3.7)$$

One can obtain the quantum field theory by promoting the wave function( $\psi$ ) to the field operator( $\Psi$ ) obeying the anti-commutation relation. Because the Schrödinger equation (3.7) is the Dirac equation in two dimensions, it is appropriate to adopt the following Lagrangian density. Addition of the electro-magnetic interaction according to the minimal coupling gives

$$\mathcal{L} = -\frac{1}{4}F^{\mu\nu}F_{\mu\nu} - \bar{\Psi}(\not{D} + M)\Psi, \quad (3.8)$$

where  $D$  is the covariant derivative and  $F_{\mu\nu}$  is the field strength,

$$\not{D} = \sum_{\mu=0,1} \left( i\hbar\partial_\mu - \frac{e}{c}A_\mu \right) \gamma^\mu, \quad (3.9)$$

$$F_{\mu\nu} = \partial_\mu A_\nu - \partial_\nu A_\mu, \quad \bar{\Psi} = \Psi^\dagger \gamma^0.$$

The gauge fields( $A_\mu$ ) live in four dimensional space-time so that summation indices run from 0 to 3 in the gauge kinetic term. We adopt the following notation:

$$g^{\mu\nu} = \text{diag}\{1, -1, -1, -1\}, \quad \gamma^0 = \begin{pmatrix} 0 & 1 \\ 1 & 0 \end{pmatrix},$$

$$\gamma^1 = \begin{pmatrix} 0 & 1 \\ -1 & 0 \end{pmatrix}, \quad \gamma^5 = -\gamma^0\gamma^1 = \begin{pmatrix} 1 & 0 \\ 0 & -1 \end{pmatrix}. \quad (3.10)$$

We quantize the fermion field in each configuration of the gauge field choosing Weyl gauge condition ( $A_0 = 0$ ). Fermionic part of the Hamiltonian density is given by

$$\mathcal{H} = \mathcal{H}_F + \mathcal{H}_C. \quad (3.11)$$

The total Hamiltonian density consists of the kinetic term and the Coulomb term. The kinetic term is given by

$$\mathcal{H}_F = \Psi^\dagger h_F \Psi$$

$$= \Psi^\dagger \begin{pmatrix} i\hbar\partial_1 - \frac{e}{c}A_1 & -M \\ -M & -(i\hbar\partial_1 - \frac{e}{c}A_1) \end{pmatrix} \Psi. \quad (3.12)$$

The Coulomb interaction term is

$$\mathcal{H}_C = \frac{e^2}{8\pi} \int \frac{J^0(x)J^0(y)}{|x-y|} dy. \quad (3.13)$$

where  $eJ^0(x)$  stands for the charge density. The electric current is given by  $eJ^\mu = e\bar{\Psi}\gamma^\mu\Psi$  where  $e$  is the electron charge.

It should be note that besides the Coulomb interaction, backscattering and umklapp process may come in the dynamics of electrons as is shown in reference [22]. We neglect these interactions providing that their coupling are weak enough.

#### IV. CHIRAL ANOMALY IN A METALLIC NANOTORUS

We have obtained the Hamiltonian density which describes the low energy excitations in the zigzag torus. The Hamiltonian consists of two parts, one is the kinetic term and the other is the Coulomb interaction. In this section we discuss the quantum mechanical vacuum structure of the kinetic Hamiltonian:  $H_F (= \int \mathcal{H}_F)$ . Effects of the Coulomb interaction will be considered in latter sections. Hereafter we focus on the metallic case:  $b = 0$ , the energy eigenvectors are given by

$$h_F \psi_n \begin{pmatrix} 1 \\ 0 \end{pmatrix} = \epsilon_n \psi_n \begin{pmatrix} 1 \\ 0 \end{pmatrix}, \quad h_F \psi_n \begin{pmatrix} 0 \\ 1 \end{pmatrix} = -\epsilon_n \psi_n \begin{pmatrix} 0 \\ 1 \end{pmatrix},$$

$$\psi_n(x) = \frac{1}{\sqrt{L}} e^{-i\frac{e}{\hbar c} \int_0^x A_1(y) dy - i\frac{\epsilon_n}{\hbar} x}, \quad (4.1)$$

where  $\epsilon_n$  is the energy eigenvalues and  $L$  is the circumferential length of the zigzag torus:  $L = 3a|M|$ . We expand the fermion field using the left and right moving waves as

$$\Psi(x, T) = \Psi_L(x, T) + \Psi_R(x, T)$$

$$= \sum_{n \in \mathbb{Z}} \left[ a_n \psi_n(x) e^{-i\frac{\epsilon_n}{\hbar} T} \begin{pmatrix} 1 \\ 0 \end{pmatrix} + b_n \psi_n(x) e^{+i\frac{\epsilon_n}{\hbar} T} \begin{pmatrix} 0 \\ 1 \end{pmatrix} \right], \quad (4.2)$$

where  $a_n, b_n$  are independent fermionic annihilation operators satisfying the anti-commutators:

$$\{a_n, a_m^\dagger\} = \{b_n, b_m^\dagger\} = \delta_{nm}. \quad (4.3)$$

All the other anticommutator vanish.

In order to get the energy spectrum  $\epsilon_n$ , we have to impose a boundary condition to the eigenfunctions. We take (2.11) as a general boundary condition. The boundary condition of the zigzag torus in the Y-direction becomes the following:

$$\hat{G}(M(2T_2 - T_1))|\Psi^k\rangle = e^{\pm i\frac{2\pi}{3}\tilde{N}}|\Psi^k\rangle, \quad (4.4)$$

where plus(minus) in exponent has its origin in the Fermi point,  $\tilde{k}_1(\tilde{k}_2)$ . Hence we should impose the following boundary conditions on the fermion energy eigenfunctions,

$$\psi_n(x + L) = e^{\pm i\frac{2\pi}{3}\tilde{N}} \psi_n(x), \quad (4.5)$$

then the energy eigenvalues are given by

$$\epsilon_n = \frac{\hbar}{L} \left[ 2\pi(n \pm \frac{\tilde{N}}{3}) - \frac{e}{\hbar c} \oint_0^L A_1 dy \right]. \quad (4.6)$$

Here, the gauge field  $A_1$  is experimentally controllable by the following experimental setup, see Fig.3. On a planar geometry we set a nanotorus and put some magnetic field inside the torus perpendicular to the plane. In this case the gauge field that expresses this magnetic field is given by, in the vector notation,  $A = \frac{N\phi_D}{2\pi}\nabla\theta$  where  $\theta$  is an angle of two points on the torus. Therefore we get a component,

$$A_1 = \frac{N\phi_D}{L}, \quad (4.7)$$

where  $\phi_D = \frac{2\pi\hbar c}{e}$ . This vector potential expresses the  $N$  flux inside the torus and by tuning the magnetic field,  $N$  can be taken as a real number.

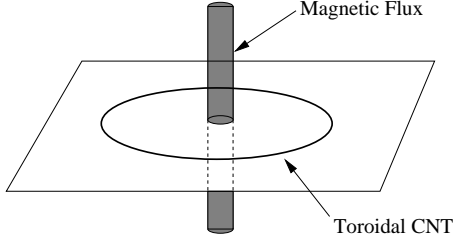


FIG. 3. A toroidal carbon nanotube on a planar geometry with magnetic field

The Lagrangian density (3.8) with massless fermion has two classical conserved currents

$$J^\mu(x) = \bar{\Psi}(x)\gamma^\mu\Psi(x), \quad (4.8)$$

$$J_5^\mu(x) = \bar{\Psi}(x)\gamma^\mu\gamma^5\Psi(x) = \epsilon^{\mu\nu}J_\nu(x), \quad (4.9)$$

where  $\epsilon^{\mu\nu}$  is an antisymmetric tensor:  $\epsilon^{01} = 1$ . Therefore, the following two charges conserve in the time evolution of the system at the classical level,

$$Q = \oint J^0(x)dx, \quad (4.10)$$

$$Q_5 = \oint J_5^0(x)dx. \quad (4.11)$$

$J^\mu$  (electric current) conservation ( $\partial_\mu J^\mu = 0$ ) is due to the gauge symmetry and  $J_5^\mu$  (chiral current) conservation ( $\partial_\mu J_5^\mu = 0$ ) is due to the global chiral symmetry ( $\Psi \rightarrow e^{i\gamma^5\alpha}\Psi$ ).

Different from classical mechanics, in the world of quantum mechanics, the chiral symmetry is broken [8]. In order to find what is happening, we need to analyze the vacuum structure:  $|vac; N_L, N_R\rangle = |vac; N_L\rangle \otimes |vac; N_R\rangle$ , where

$$|vac; N_L\rangle = \prod_{n=-\infty}^{N_L-1} a_n^\dagger|0\rangle, \quad |vac; N_R\rangle = \prod_{N_R}^{n=\infty} b_n^\dagger|0\rangle. \quad (4.12)$$

We define  $|vac; N_L\rangle(|vac; N_R\rangle)$  such that the levels with energy lower than  $\epsilon_{N_L}(-\epsilon_{N_R-1})$  are filled and the others are empty. On this vacuum the charge expectation values and the energy become

$$\langle Q \rangle = N_L - N_R, \quad (4.13)$$

$$\langle Q_5 \rangle = N_L + N_R - 2N - 1 \pm \frac{2}{3}\tilde{N}, \quad (4.14)$$

$$\langle H_F \rangle = \frac{2\pi\hbar}{L} \left( \frac{\langle Q \rangle^2 + \langle Q_5 \rangle^2}{4} - \frac{1}{12} \right). \quad (4.15)$$

To obtain the above results, we have regularized the divergent eigenvalues on the vacuum by  $\zeta$ -function regularization, for example, the gauge charge is regularized as follows:

$$Q = \lim_{s \rightarrow 0} \left( \sum_{n \in \mathbb{Z}} a_n^\dagger a_n \frac{1}{|\lambda\epsilon_n|^s} + \sum_{n \in \mathbb{Z}} b_n^\dagger b_n \frac{1}{|-\lambda\epsilon_n|^s} \right), \quad (4.16)$$

where  $\lambda$  is an arbitrary constant with dimension of length which is necessary to make  $\lambda\epsilon_n$  dimensionless. This regularization respects gauge invariance because the energy of each level is a gauge invariant quantity.

It can be shown that the gauge charge  $\langle Q \rangle$  must vanish in order that the state is a physical state. We now have  $N_L = N_R$ . From the above equation (4.14), it can be seen that if  $N_L$  and  $N_R$  are conserved, then, by varying  $N$  (the magnetic field), the chiral charge also changes. Therefore it is not a conserved quantity. We thus see that the vacuum is responsible for non-conservation of chirality even though the dynamics is chirally invariant. From eq.(4.9) we see that the chiral current  $J_5^0$  is equivalent to the electric current in the tubule axis direction,

$$Q_5 = \oint J_5^0(x)dx = - \oint J^1(x)dx = -J^1. \quad (4.17)$$

Hence, in order to observe the anomaly, we should observe the electrical current in the torus.

Due to the existence of the two Fermi points, the total current in the torus is given by the sum of two currents  $\langle Q_5 \rangle_{\tilde{k}_1}$  and  $\langle Q_5 \rangle_{\tilde{k}_2}$ . We should care for the sign( $\pm$ ) in the chiral charge (4.14). We define

$$\langle Q_5 \rangle_{\tilde{k}_1} = N_L + N_R - 2N - 1 + \frac{2}{3}\tilde{N}, \quad (4.18)$$

$$\langle Q_5 \rangle_{\tilde{k}_2} = N_L + N_R - 2N - 1 - \frac{2}{3}\tilde{N}, \quad (4.19)$$

and treat them separately.

It is clear from the above equations that there are two origins of the usual current flow in the torus. One is the  $N_L + N_R$  term which can be induced in thermal bath or by a sudden change of the magnetic field. On the other hand, magnetic field can change the quantum vacuum structure and lead to the anomaly. In order to avoid the unexpected changes of  $N_L (= N_R)$ , the magnetic field must be changed adiabatically at low temperature ( $< \frac{2\pi\hbar}{L}$ ). However, in the adiabatic process, when the strength of the magnetic field reaches the specific points, then  $N_L (= N_R)$  also have to change. For simplicity, we set  $\tilde{N} = 1$  and focus on the  $\langle Q_5 \rangle_{\tilde{k}_1}$ . When increasing  $N$  starting from the point  $N = 0, N_L = 0$ , the energy is going up as in eq(4.15). At  $N = \frac{1}{3}$ , the spectrum meets an another line of spectrum  $N_L = 1$ , see Fig.4. Therefore the circular current for  $\tilde{k}_1$  in the ring

$$J^1(\tilde{k}_1) = 2(N - N_L) + \frac{1}{3} \quad (4.20)$$

follows the line shown in Fig.5.

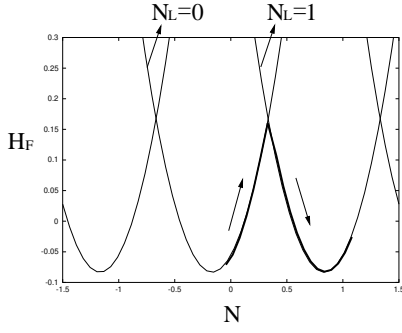


FIG. 4. Adiabatic change of the fermionic energy of  $\tilde{k}_1$  point. The energy value is labeled in the unit of  $\frac{2\pi\hbar}{L}$

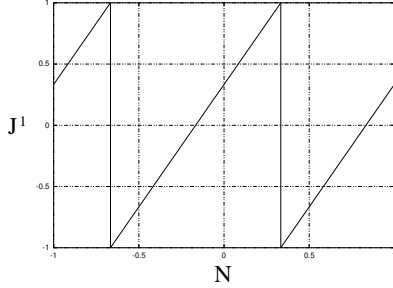


FIG. 5. Induced current in the twisted zigzag torus:  $J^1(\tilde{k}_1) = -\langle Q_5 \rangle_{\tilde{k}_1}$

The same analysis can be applied to the case of  $J^1(\tilde{k}_2) = -\langle Q_5 \rangle_{\tilde{k}_2}$ , the adiabatic change of energy and induced current are shown in Fig.6 and Fig.7.

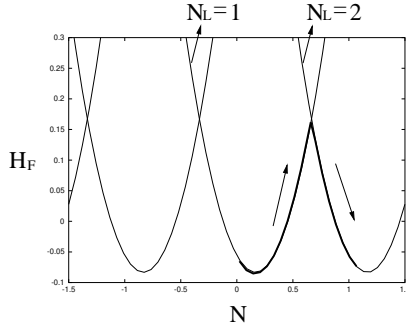


FIG. 6. Adiabatic change of the fermionic energy of  $\tilde{k}_2$  point. The energy value is labeled in the unit of  $\frac{2\pi\hbar}{L}$

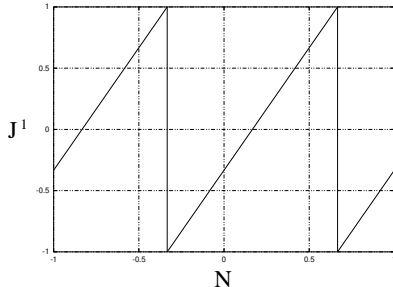


FIG. 7. Induced current in the twisted zigzag torus:  $J^1(\tilde{k}_2) = -\langle Q_5 \rangle_{\tilde{k}_2}$

Total current on the torus is given by a sum of two current,

$$J = J^1(\tilde{k}_1) + J^1(\tilde{k}_2). \quad (4.21)$$

Magnetic field dependence of the total current is shown in Fig.8. Dotted line in Fig.8 indicates the current on the untwisted ( $\tilde{N} = 0$ ) torus. At each Fermi point, there are two spin degrees of freedom. Therefore the actual current is twice the  $J$ . This current for untwisted torus shows the same magnetic field dependence to the persistent current in ref. [14].

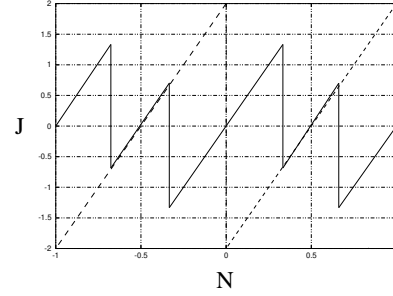


FIG. 8. Magnetic field dependence of the total current on the torus:  $J = J^1(\tilde{k}_1) + J^1(\tilde{k}_2)$

## V. VACUUM STRUCTURE OF A CARBON NANOTORUS

In this section we consider the vacuum structure of the total Hamiltonian:

$$H = \oint \mathcal{H} = H_F + H_C, \quad (5.1)$$

$$H_C = \frac{e^2}{8\pi c} \oint \frac{J^0(x)J^0(y)}{|x-y|} dx dy.$$

In the previous section we have solved the kinetic part of the total Hamiltonian. We clarified its vacuum state and obtained the regularized eigenvalues of the physical quantities. We saw that the vacuum has the chiral charge so that it read the chiral anomaly. What we are interested in at this point is whether the previous results change or not by the inclusion of the Coulomb interaction in our analysis [11]. Furthermore we hope to make clear the effects of the ‘external’ charge density on the chiral anomaly. Their understandings are the first step for studying more physically interesting situations such as impurity effect, CNT-CNT junction or junctions of a CNT and a metal or a superconductor.

The Coulomb interaction consists of a product of the charge density. Therefore it is very convenient to rewrite the kinetic term  $H_F$  using the current operators. For this purpose, it is useful to introduce the left and right currents as follows:

$$J^0(x) = J_L(x) + J_R(x), \quad (5.2)$$

where  $J_L(x) = \Psi_L^\dagger(x)\Psi_L(x)$  and  $J_R(x) = \Psi_R^\dagger(x)\Psi_R(x)$ . We expand these currents by the Fourier modes,

$$J_L(x) = \sum_{n \in \mathbb{Z}} \frac{j_L^n}{L} e^{-i \frac{2\pi n x}{L}}, \quad J_R(x) = \sum_{n \in \mathbb{Z}} \frac{j_R^n}{L} e^{+i \frac{2\pi n x}{L}}, \quad (5.3)$$

where the Fourier components are the bosonic operators,

$$j_L^n = \sum_{m \in \mathbb{Z}} a_m^\dagger a_{m+n}, \quad j_R^n = \sum_{m \in \mathbb{Z}} b_{m+n}^\dagger b_m, \quad (5.4)$$

which satisfy the following commutation relations on the fermion Fock space,

$$[j_L^n, (j_L^m)^\dagger] = n \delta_{n,m}, \quad (5.5)$$

$$[j_R^n, (j_R^m)^\dagger] = n \delta_{n,m}. \quad (5.6)$$

It is well-known that the following Hamiltonian has the same matrix element as the original fermion Hamiltonian:

$$H_F = \frac{2\pi\hbar}{L} \left\{ \left( \frac{Q^2 + Q_5^2}{4} - \frac{1}{12} \right) + \sum_{n>0} ((j_L^n)^\dagger j_L^n + (j_R^n)^\dagger j_R^n) \right\}. \quad (5.7)$$

This Hamiltonian has a new term which is not shown in eq.(4.15). This term has vanishing value on the previous vacuum state because

$$j_L^n |vac; N_L\rangle = 0, \quad j_R^n |vac; N_R\rangle = 0, \quad (5.8)$$

for positive  $n$ .

The Coulomb interaction can be rewritten using the bosonic current operators,

$$H_C = \frac{e^2}{4\pi Lc} \sum_{n \geq 0} V(n) ((j_L^n)^\dagger + j_R^n) (j_L^n + (j_R^n)^\dagger). \quad (5.9)$$

Here, we introduce the Fourier component of the Coulomb potential,

$$V(n) = 2\pi \int_0^1 dz \frac{\cos(2\pi n z)}{\sqrt{\sin^2(\pi z) + \left(\frac{R}{L}\right)^2}}, \quad (5.10)$$

where  $R$  is the circumference of the tubule.

Some comments are in order. When we write the Coulomb interaction in eq.(5.1), it has an ultraviolet divergence in the limit of  $x \rightarrow y$ . Therefore we need to introduce some cutoff length. It is appropriate that we set it the length of a diameter of a tubule because we make the approximation that mixing of the different momentums in the compactified direction cannot happen. This explain the  $\left(\frac{R}{L}\right)^2$  term in the denominator. Besides, the form of a torus is not a line but a ring on a plane so that we should use the direct length between  $x$  and  $y$  in the Coulomb interaction. This is the origin of the  $\sin^2(\pi z)$  term in the denominator.

We combine the kinetic term and the Coulomb term as follows:

$$H = H_0 - \frac{2\pi\hbar}{12L} + \sum_{n>0} H_n, \quad (5.11)$$

where

$$H_0 = \frac{2\pi\hbar}{L} \frac{Q_5^2 + \kappa Q^2}{4}, \quad \kappa = 1 + \frac{\alpha}{\pi} V(0), \quad (5.12)$$

and

$$H_n = \frac{2\pi\hbar}{L} \{ (j_L^n)^\dagger j_L^n + j_R^n (j_R^n)^\dagger - n \} + \frac{e^2 V(n)}{4\pi Lc} ((j_L^n)^\dagger + j_R^n) (j_L^n + (j_R^n)^\dagger). \quad (5.13)$$

Here we introduce the fine structure constant  $\alpha (= \frac{e^2}{4\pi\hbar c})$ .

We diagonalize the Hamiltonian  $H_n (n \neq 0)$  using the Bogoliubov transformation:

$$\begin{pmatrix} \tilde{j}_L^n \\ (\tilde{j}_R^n)^\dagger \end{pmatrix} = \begin{pmatrix} \cosh t_n & \sinh t_n \\ \sinh t_n & \cosh t_n \end{pmatrix} \begin{pmatrix} j_L^n \\ (j_R^n)^\dagger \end{pmatrix}, \quad (5.14)$$

where

$$\sinh 2t_n = \frac{1}{E_n} \frac{e^2 V(n)}{4\pi Lc}, \quad (5.15)$$

$$\cosh 2t_n = \frac{1}{E_n} \left( \frac{2\pi\hbar}{L} + \frac{e^2 V(n)}{4\pi Lc} \right), \quad (5.16)$$

$$E_n = \frac{2\pi\hbar}{L} \sqrt{1 + \frac{\alpha}{\pi} V(n)}. \quad (5.17)$$

After some calculations we derive

$$H_n = E_n [(\tilde{j}_L^n)^\dagger \tilde{j}_L^n + (\tilde{j}_R^n)^\dagger \tilde{j}_R^n + n] - \frac{2\pi\hbar}{L} n. \quad (5.18)$$

The energy  $E_n$  differs from  $\frac{2\pi\hbar}{L}$ . The difference is due to the Coulomb interaction and is small owing to the factor  $\frac{\alpha}{\pi}$ , see Fig.9.

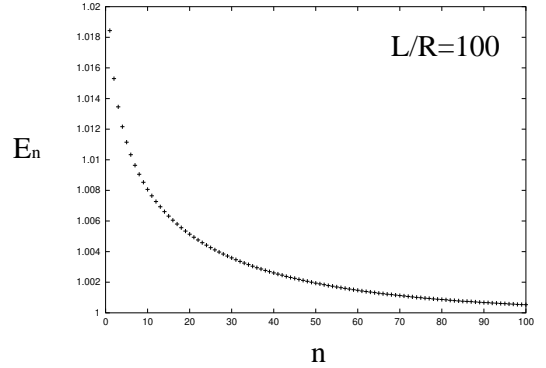


FIG. 9. Energy spectrums are corrected slightly by the Coulomb interaction. The energy value is labeled in the unit of  $\frac{2\pi\hbar}{L}$ . Here we set  $\frac{L}{R} = 10^2$  in eq.(5.10).

The generators of the Bogoliubov transformation are given by

$$U_n = \exp \left( -\frac{t_n}{\sqrt{2n}} \{ (\tilde{j}_L^n)^\dagger (\tilde{j}_R^n)^\dagger - \tilde{j}_L^n \tilde{j}_R^n \} \right). \quad (5.19)$$

Hence, we obtain the vacuum state as follows:

$$|\widetilde{vac}\rangle = \left( \prod_{n>0} U_n \right) |vac; N_L, N_R\rangle, \quad (5.20)$$

where  $N_L = N_R$ . The previous vacuum state changes into new vacuum by the Coulomb interaction. We should estimate

the gauge charge and chiral charge on this new vacuum. Because the operators  $(U_n)$  commute with the charge operators  $Q$  and  $Q_5$ , the eigenvalues of these charges do not change.

$$Q|\widetilde{vac}\rangle = 0, \quad (5.21)$$

$$Q_5|\widetilde{vac}\rangle = \left(2(N_L - N) - 1 \pm \frac{\tilde{N}}{3}\right)|\widetilde{vac}\rangle. \quad (5.22)$$

Hence, the chiral anomaly which we have considered in the previous section still exists when we include the Coulomb interaction into the analysis [11].

## VI. EFFECTS OF EXTERNAL CHARGES

We have so far considered the Coulomb interaction between the internal charges. However, more important problem may be the following: when we put external charges on a nanotorus, how the vacuum structure change? A fixed external charge may corresponds to an electrical contact or an impurity on a torus. In this section we put external charges on a torus and study the vacuum structure. Especially we analyze an effect of external charges on the chiral charge, the potential behavior between a pair of external charges and the ‘charge screening’ effect. The charge screening means that the internal charge density is induced by the external charges so that the external charges are screened.

We set two unit external charges on a torus. One has a unit charge  $e$  placed at  $x_0$  and the other has an opposite charge  $-e$  at  $y_0$ .

$$\begin{aligned} J_{ex}^0(x) &= \delta(x - x_0) - \delta(x - y_0) \\ &= \frac{1}{L} \sum_{n \in Z} j_{ex}^n e^{-i \frac{2\pi n x}{L}}, \end{aligned} \quad (6.1)$$

where

$$j_{ex}^n = e^{i \frac{2\pi n x_0}{L}} - e^{i \frac{2\pi n y_0}{L}}. \quad (6.2)$$

We consider the Coulomb interaction with the following charge density which is a sum of the internal charges and the external charges:

$$\begin{aligned} J^0(x) + J_{ex}^0(x) &= \\ &= \sum_{n \in Z} \left( (\tilde{j}_L^n)^\dagger + j_R^n + (j_{ex}^n)^* \right) \frac{1}{L} e^{i \frac{2\pi n x}{L}}. \end{aligned} \quad (6.3)$$

After some calculations we get

$$\begin{aligned} H_n(J_{ex}) &\equiv E_n \left[ \left( (\tilde{j}_L^n)^\dagger + \gamma_n (j_{ex}^n)^* \right) (\tilde{j}_L^n + \gamma_n j_{ex}^n) \right. \\ &\quad \left. + \left( (\tilde{j}_R^n)^\dagger + \gamma_n j_{ex}^n \right) (\tilde{j}_R^n + \gamma_n (j_{ex}^n)^*) + n \right] \\ &\quad - \frac{2\pi\hbar}{L} n + \frac{\beta_n}{E_n^2} \left( \frac{2\pi\hbar}{L} \right)^2 (j_{ex}^n)^* j_{ex}^n, \end{aligned} \quad (6.4)$$

where  $\gamma_n = \sinh 2t_n (\cosh t_n - \sinh t_n)$  and  $\beta_n = \frac{e^2}{4\pi L c} V(n)$ . It is easy to find conditions of the vacuum in the presence of the external charges,

$$(\tilde{j}_L^n + \gamma_n j_{ex}^n) |\widetilde{vac}; J_{ex}^0\rangle = 0, \quad (6.5)$$

$$(\tilde{j}_R^n + \gamma_n (j_{ex}^n)^*) |\widetilde{vac}; J_{ex}^0\rangle = 0, \quad n > 0. \quad (6.6)$$

First we can easily show that the chiral charge on this new vacuum does not change even in the presence of external charges,

$$\langle \widetilde{vac}; J_{ex}^0 | J^5(x) | \widetilde{vac}; J_{ex}^0 \rangle = \frac{\langle Q_5 \rangle}{L}. \quad (6.7)$$

So, the current by the chiral anomaly is not affected by the charged impurities. Second, we estimate the energy change due to the presence of the external charges:

$$\begin{aligned} E(x_0 - y_0) &= \langle \widetilde{vac}; J_{ex}^0 | H(J_{ex}) | \widetilde{vac}; J_{ex}^0 \rangle - \langle \widetilde{vac} | H | \widetilde{vac} \rangle \\ &= \sum_{n>0} \frac{\beta_n}{E_n^2} \left( \frac{2\pi\hbar}{L} \right)^2 (j_{ex}^n)^* j_{ex}^n \\ &= \frac{2\pi\hbar}{L} \sum_{n>0} \frac{\frac{\alpha}{\pi} V(n)}{1 + \frac{\alpha}{\pi} V(n)} \left( 1 - \cos \frac{2\pi n(x_0 - y_0)}{L} \right), \end{aligned} \quad (6.8)$$

where  $H(J_{ex})$  is the Hamiltonian with the external charges  $(J_{ex})$ . This energy may be approximated by

$$E(x_0 - y_0) \simeq \alpha \frac{2\pi\hbar}{R} \left( 1 - \frac{1}{\sqrt{1 + \left( \frac{\pi(x_0 - y_0)}{R} \right)^2}} \right). \quad (6.9)$$

Fig.10 shows the potential energy (eq.(6.8)) as a function of the distance between the two external charges.

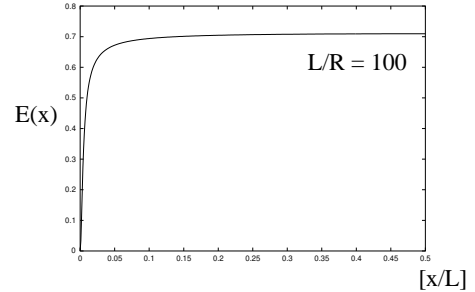


FIG. 10. Distance dependence of the energy caused by two fixed external charges. The energy value is labeled in the unit of  $\frac{2\pi\hbar}{L}$ . The distance between two external charges is scaled by  $L$ . Here we take  $\frac{L}{R} = 10^2$  in eq.(5.10).

We see that the effect of the ‘charge screening’ on the external charge can be ignored in a metallic nanotorus. Because the potential energy is now shown to be long-ranged. This means that even if some internal charges are influenced by the external charges, the quantity of the induced charges should be very small. To confirm this, we also compute the induced internal charges distribution,

$$\langle \widetilde{vac}; J_{ex}^0 | J^0(x) | \widetilde{vac}; J_{ex}^0 \rangle = f(x; x_0) - f(x; y_0), \quad (6.10)$$

where

$$f(x; x_0) = -\frac{2}{L} \sum_{n>0} \frac{\frac{\alpha}{\pi} V(n)}{1 + \frac{\alpha}{\pi} V(n)} \cos \frac{2\pi n(x - x_0)}{L}. \quad (6.11)$$

This function is displayed in Fig.11. It is clear that the induced charge density is very small. Hence, the charge screening effect is incomplete.

We should stress here that the above analysis on the charging energy (6.8) and screening (6.11) are not complete because



the charge density ( $J^0(x)$ ) in the Coulomb interaction consist of one massless fermion in our analysis. A CNT have four independent fermions due to the two Fermi points(2.18) and spin degrees of freedom. However, straight forward extension of our analysis shows that the charging energy hardly changes and the screening effect is about four times larger than the above result [23]. Therefore the conclusions in this paper are still valid.

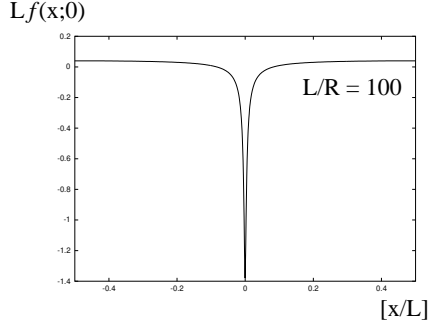


FIG. 11. The internal charge density modulation around a unit charge  $e$  placed at origin:  $f(x, 0)$ . The charge density value and the distance from the charge are labeled in the unit of  $L$  and  $\frac{1}{L}$  respectively. Here we take  $\frac{L}{R} = 10^2$  in eq.(5.10).

## VII. CONCLUSION AND DISCUSSION

In this paper we analyzed the carbon nanotorus and discussed the quantum mechanical vacuum structure of a metallic torus. The significance of our present work may be put as follows.

We used the quantum field theory to analyze the vacuum structure of a metallic nanotorus. We pointed out that the chiral anomaly in 1+1 dimensions should be observed in the form of specific magnetic field dependence to the current. This current is the same as the persistent current. It is certain that the persistent current can be understood in the light of the chiral anomaly in 1+1 dimensions. We also clarified the vacuum state including the Coulomb interaction and discussed the effect of ‘charge screening’ on the external charges. It was found that the chiral anomaly is not affected by the charged impurities and the charge screening effect is negligibly small. From this observation, we conclude that the interaction between external charges and charged impurities is long-range Coulomb interaction. This is to be contrasted with the screening effect for the massless Schwinger model [11].

Although we have analyzed a nanotorus in the present paper, we can regard the torus as a tube locally provided the circumferential length of the torus is large. Hence, we may apply the results obtained in the analysis of the torus to the study of a carbon nanotube. To take an example, it is reasonable to suppose that the screening effect is also negligible on a tube like a torus.

What we do not consider in this paper are effects of finite temperature ( $> \frac{2\pi\hbar}{L}$ ) on chiral anomaly and screening of external charges. In finite temperature, in addition to the electron field, phonon field would come into play [24]. This phonon field may be vital to understand the electrical behavior of the carbon nanotube at finite temperature. We would

like to make a quantitative analysis of finite temperature effects in a future report.

## VIII. ACKNOWLEDGMENTS

The author would like to thank M. Hashimoto for various discussions on the subject. This work is supported by a fellowship of the Japan Society of the Promotion of Science.

- 
- [1] S. Iijima, *Nature*, **354**, 56 (1991).
  - [2] R. Saito, G. Dresselhaus and M.S. Dresselhaus, *Physical Properties of Carbon Nanotubes* (1998) Imperial College Press, London.
  - [3] *The Science and Technology of Carbon Nanotubes* (1999) Ed. by K. Tanaka, T. Yamabe and K. Fukui, Elsevier Oxford.
  - [4] C. Dekker, *Phys. Today* **52**, No. 5, 22 (1999).
  - [5] J.W. Mintmire, B.I. Dunlap and C.T. White, *Phys. Rev. Lett.* **68**, 631 (1992); N. Hamada, S. Sawada and A. Oshiyama, *Phys. Rev. Lett.* **68**, 1579 (1992); R. Saito et al., *Appl. Phys. Lett.* **60**, 2204 (1992).
  - [6] J. W. G. Wildöer et al., *Nature*, **391**, 59 (1998); T. W. Odom et al., *Nature*, **391**, 62 (1998).
  - [7] J. Liu et al. *Nature*, **385**, 781 (1997).
  - [8] J.S. Bell and R. Jackiw, *Nuovo Cim.* **60**, 47 (1969); S. Adler, *Phys. Rev.* **177**, 2426(1969).
  - [9] J. Schwinger, *Phys. Rev.* **128**, 2425 (1962); J. Lowenstein and A. Swieca, *Ann. Phys.* **68**, 172 (1971).
  - [10] The massless Schwinger model (quantum electrodynamics with massless fermion in one spatial dimension) is first solved in the Hamiltonian formalism by, N. S. Manton, *Ann. Phys.* **159**, 220 (1985).
  - [11] Most of the detail about the massless Schwinger model can be found in, S. Iso and H. Murayama, *Prog. Theor. Phys.* **84**, 142 (1990).
  - [12] R. Jackiw, in: *Lectures on current algebra and its applications*, eds. S. Treiman, R. Jackiw and D. Gross, Princeton Univ. Press, Princeton, (1972).
  - [13] H.B. Nielsen and M. Ninomiya, *Phys. Lett.* **130B**, 389 (1983); I. Krive and A. Rozhavsky, *Phys. Lett.* **113A**, 313 (1983); M. Stone and F. Gaitan, *Ann. Phys. (NY)* **178**, 89 (1987).
  - [14] The persistent current in toroidal carbon nanotubes is analyzed by, R.C. Haddon, *Nature*, **388**, 31 (1997); M.F. Lin, *Phys. Rev. B.* **57**, 6731 (1998); A.A. Odintsov, W. Smit and H. Yoshioka, *Europhys. Lett.*, **45**, 598 (1999).
  - [15] J. González, F. Guinea and M.A.H. Vozmediano, *Nucl. Phys.* **B406**, 771 (1993).
  - [16] Y. -K. Kwon and D. Tománek, *Phys. Rev. B.* **58**, R16001 (1998).
  - [17] P. Kim et al., *Phys. Rev. Lett.* **82**, 1225 (1999). An experimental result suggests that curvature-induced hybridization is only a small perturbation for the (13,7) tube.

- [18] W. Clauss, D. J. Bergeron and A. T. Johnson, Phys. Rev. B. **58**, R4266 (1998).
- [19] It should be noted that to obtain eq.(2.19) we have to perturb the Hamiltonian around the points  $a\tilde{k}_1 - aK_1$  and  $a\tilde{k}_2 + aK_1$ . The wave vectors  $K_i$  satisfy the conditions,  $K_i \cdot T_j = 2\pi\delta_{ij}$ . The vectors  $a\tilde{k} \pm aK_1$  and  $a\tilde{k}$  represent the same state since any two wave vectors congruent by  $aK_i$  are just different labels of the same state.
- [20] D. P. DiVincenzo and E. J. Mele, Phys. Rev. B **29**, 1685 (1984); H. Ajiki and T. Ando, Solid. State. Commun. **102**, 135 (1997); T. Ando and T. Nakanishi, J. Phys. Soc. Jpn. **67**, 1704 (1998).
- [21] In order to get the unnormalized energy we should multiply  $\beta$  by  $\epsilon_n$ . We estimate the order of magnitude of energy spectrum using  $\beta \sim \frac{c}{400}$ . Here we use  $\gamma = 2.5[\text{eV}]$  and  $a = 1.42[\text{\AA}]$ ,  $\beta\epsilon_n \sim 5(\text{eV}) \left[ \frac{\text{\AA}}{L} \right] 2\pi(n - N)$ .
- [22] R. Egger and A.O. Gogolin, Phys. Rev. Lett., **79**, 5082 (1997).
- [23] K. Sasaki, work in progress.
- [24] B. Sakita and K. Shizuya, Phys. Rev. B. **42**, 5586 (1990).